

Improvement of Geant4 Neutron-HP package: Doppler broadening of the neutron elastic scattering kernel and cross sections

M. Zmeškal^{a,b,*}, L. Thulliez^c, E. Dumonteil^c

^a*Dept. of Nuclear Reactors, Faculty of Nuclear Sciences and Physical Engineering, Czech Technical University in Prague, V Holesovickach 2, Prague, 180 00, Czech Republic*

^b*Research Centre Rez, Hlavní 130, Husinec-Rez, 250 68, Czech Republic*

^c*Université Paris-Saclay, CEA, Institut de Recherche sur les Lois Fondamentales de l'Univers, 91191, Gif-sur-Yvette, France*

Abstract

Whether it is for shielding applications or for safety criticality studies, numerically solving the neutron transport equation with a good accuracy requires to precisely estimate the Doppler broadened elastic scattering kernel in the thermal and epithermal energy range of neutrons travelling in a free gas. In Geant4, low energy neutrons are transported using evaluated data libraries handled by the Neutron High-Precision (Neutron-HP) package. Version 11.00.p03 of the code features in particular the Doppler broadened elastic scattering kernel, provided by the so-called 'Sampling of the Velocity of the Target' (SVT) method. However this latter fails for resonant heavy nuclei such as ^{238}U and can severely impact the solving of the Boltzmann equation in fissile media. To overcome this shortcoming, the Doppler Broadened Rejection Correction (DBRC) method has been implemented in Geant4 and successfully validated with the reference Monte Carlo neutron transport code Tripoli-4[®] (version 11). This development will be taken into account in the next release of the code. The cross section Doppler broadening process, which is performed on-the-fly, is also carefully investigated and ways to improve it on a simulation-by-simulation basis are presented. All the validations have been performed with an automated benchmark tool which has been designed to support the quality assurance of the Geant4 Neutron-HP package. This tool is currently available on an ad hoc Gitlab repository and will be included in Geant4.

Keywords:

Geant4, Neutron-HP, Neutron elastic scattering kernel, Doppler broadening, DBRC, Tripoli-4[®]

1. Introduction

Monte Carlo codes are routinely used for particle transport applications since they allow to track particles individually and eventually to keep correlations between them. To this aim the Geant4 open-source toolkit has been developed by an international collaboration with the aim of supporting high-energy physics applications, as well as other domains, like space science, medical physics, engineering and nuclear physics.[1, 2, 3]. In the past decades, the Geant4 physics range has been extended to lower energies, including low energy neutron transport (*i.e.* below 20 MeV) through the development of the Neutron High-Precision (Neutron-HP) package which is mainly based on evaluated nuclear data libraries to accurately describe neutron-matter interactions. During the last years in particular, the Neutron-HP package has been gradually improved [4, 5, 6, 7], due to the increasing need for neutron transport capabilities in the broader context of multi-particle transport codes required by applications such as accelerator physics, medical imaging and radiotherapy, fundamental physics, nuclear industry, etc. These latest Geant4 developments place the code close to be on-par with reference neutron transport codes such as Tripoli-4[®] [8] or MCNP6 [9].

*Corresponding author

Email addresses: zmeskma1@jfji.cvut.cz (M. Zmeškal), loic.thulliez@cea.fr (L. Thulliez)

Neutron transport simulations heavily rely on an accurate description of neutron-matter interactions and more specifically on a proper handling of the temperature of the material in which the neutron propagate because low energy neutrons (thermal and epithermal) are sensitive to molecular and atomic thermal motions. This latter cannot usually be neglected during neutron transport since it affects both the cross section and the final state of the reactions. Indeed the available energy in the centre of mass of the system depends on the relative velocity between the neutron and the moving target nucleus. This effect gives rise to the Doppler broadening process which can be written as:

$$\sigma_T(v_n) = \frac{1}{v_n} \int v_r \sigma_{T=0K}(v_r) \mathcal{M}(\mathbf{V}_t, T) d\mathbf{V}_t \quad (1)$$

with σ_T the Doppler broadened cross section at temperature T , $\mathcal{M}(\mathbf{V}_t, T)$ the target velocity distribution, $v_r = \|\mathbf{v}_n - \mathbf{V}_t\|$ the relative velocity between the neutron, \mathbf{v}_n , and the target nucleus, \mathbf{V}_t . The cross section Doppler broadening can be performed exactly for example with the SIGMA-1 algorithm [10]. The definition of the final state of the reaction has to be coherent with the Doppler broadened cross section value. Often in Monte Carlo neutron transport codes the final state definition is divided in three domains depending on the neutron energy E_n , as sketched in Figure 1. For $E_n > \text{SVT_E_max}$, with $\text{SVT_E_max} = 400 k_B T$ (~ 10.5 eV at 300 K) and k_B the Boltzmann constant, the target nuclei are considered at rest, leading to the use of the so-called 0 K asymptotic elastic scattering kernel. For $E_n < \text{SVT_E_max}$, the target nuclei are assumed to behave as a free gas, *i.e.* moving freely relative to each other, and are described by a Maxwellian velocity distribution which is a valid approximation for many targets (in particular metallic), therefore in the following $\mathcal{M}(\mathbf{V}_t, T)$ is set to be a Maxwell-Boltzmann distribution. The final state is then derived from Equation 1 assuming a constant cross section over the relative velocity range leading to the so called 'Sampling of the Velocity of the Target' (SVT) method. Furthermore if the molecular and atomic bonds have a significant impact, *i.e.* for $E_n < \text{S}(\alpha, \beta)_E_max$ with $\text{S}(\alpha, \beta)_E_max = 4$ eV in Geant4, the free gas model does not hold true anymore and $\text{S}(\alpha, \beta)$ tables grasping the complex underlying physics of neutron-molecule or neutron-atom interactions have to be used to compute both the cross sections and scattering kernels. These tables are available for most materials used in nuclear reactor physics such as light water or uranium dioxide, since it can significantly impact the simulation predictions.

The SVT assumption used to compute the final state for $E_n < \text{SVT_E_max}$ is not valid for resonant heavy nuclei since their cross sections vary rapidly by a few orders of magnitude over a narrow energy range. To overcome this shortcoming, after a presentation in Section 2 of the tools used in this work, in Section 3 the Doppler Broadening Rejection Correction (DBRC) algorithm implementation and validation in Geant4 are presented. Then in Section 4 the on-the-fly cross section Doppler broadening process in Geant4 is carefully studied and improvements are suggested.

2. Benchmark methodology and tools

The developments performed in this work have been done with Geant4 version 11.00.p03. The results are compared to the reference neutron transport codes Tripoli-4[®] (version 11) and MCNP6 (version 6.2). Tripoli-4[®] is developed since the mid-1990s at CEA-Saclay (France) and is used as a reference code by the main French nuclear companies [8]. MCNP6 is developed at Los Alamos National Laboratory (United States) and is used worldwide as a reference neutron transport code for many applications involving neutrons. Both codes are used for criticality-safety system studies, depletion calculations and shielding applications. They benefit from a very large verification and validation database gathering more than 1000 experimental benchmarks and are regularly validated/qualified using inter-code comparisons [11]. The evaluated data library ENDF/B-VII.1 [12] is used in this work through the G4NDL4.5 library in Geant4.

In the following, the developments performed in Geant4 are validated with a differential-microscopic benchmark referred to as the thin-cylinder benchmark [4, 7]. Its geometry is a thin cylinder with a radius $r = 1 \mu\text{m}$ and a length $L = 2$ m. Mono-energetic neutrons, with a mean free path λ_n , are shot along the cylinder axis. The cylinder dimensions are chosen to have at least one collision ($\lambda_n \ll L$) and to ensure

that only one collision will occur in the cylinder ($r \ll \lambda_n$). The neutron characteristics after the collision are tallied such as energy, angle, etc. It has to be mentioned that this thin-cylinder benchmark is a part of a broader set of automated benchmarks, which also includes an integral-macroscopic benchmark called the sphere benchmark in which the neutron flux is tallied within a 30 cm radius sphere having a mono-energetic and isotropic source at its center [7]. These automated benchmarks have been developed to test and assess the quality of new Geant4 releases with respect to its Neutron-HP package. In this framework, once the Geant4 simulations are performed, this tool compares the Geant4 results to Tripoli-4[®] or MCNP6 results aggregated in a database and tests the statistical significance of the results to alert on potential problems. Finally it outputs a report summarising the results. This code is made available to the community on the following Gitlab repository [13] and will be included to Geant4.

In this work, the thin-cylinder material is set to ^{238}U because it has low energy resonances in its cross sections. The primary neutron energies are chosen to be below the first three resonances, *i.e.* at 6.52 eV, 20.2 eV and 36.25 eV. The temperature effects on the elastic scattering kernels have been investigated with the ^{238}U material set at 300 K, 600 K and 1000 K. For each temperature-energy combination 10^8 neutrons are simulated.

3. Doppler broadened neutron elastic scattering kernel

3.1. Study of the SVT algorithm for heavy nuclei

The effect of thermal motion on the final state definition is mainly important for elastic scattering, because it is a non-threshold and non-absorbing reaction. Therefore in many neutron transport codes the SVT algorithm is just applied to elastic scattering whereas in Geant4 it is applied to all reaction channels (elastic, capture, etc). In the following only the elastic scattering reaction is considered.

The target nucleus thermal motion changes the outgoing neutron energy and scattering angle probabilities. To take it into account, the sampling of the velocity of the target nucleus \mathbf{V}_t has to be done in a way that preserves the reaction rate given by Equation 1 [14]. This sampling can be transformed into a selection of the pair (μ, V_t) , where μ is the cosine of the angle between the neutron and target nucleus velocities. By introducing the exact form of $\mathcal{M}(\mathbf{V}_t, T)$ into Equation 1 and integrating it over the azimuthal angle, the following joint probability distribution can be written:

$$p(V_t, \mu)dV_t d\mu = \frac{v_r \sigma_0(v_r) \frac{\beta^3}{\pi^{\frac{3}{2}}} V_t^2 e^{-\beta^2 V_t^2} 2\pi}{v_n \sigma_T(v_n)} dV_t d\mu \quad (2)$$

with $\beta = \sqrt{\frac{M}{2k_B T}}$ and M the target mass. In this distribution μ and V_t are correlated and cannot be sampled independently. When the assumption is made that $\frac{\sigma_0(v_r)}{\sigma_T(v_n)}$ is constant over the relative velocity range v_r , the SVT joint probability distribution is obtained:

$$p_{\text{SVT}}(V_t, \mu)dV_t d\mu = C \underbrace{\frac{d\mu}{2}}_{(A)} \underbrace{(v_n + V_t) \frac{4\beta^3}{\sqrt{\pi}} V_t^2 e^{-\beta^2 V_t^2} dV_t}_{(B)} \underbrace{\left(\frac{v_r}{v_n + V_t} \right)}_{(C)} \quad (3)$$

In the SVT algorithm, μ is firstly sampled uniformly between $[-1, 1]$. Then in sampling V_t from (B), V_t is sampled from $\frac{4\beta^3}{\sqrt{\pi}} V_t^2 e^{-\beta^2 V_t^2} dV_t$ with probability $P_1 = \frac{v_n}{v_n + \sqrt{\pi}\beta}$ and then from $2\beta^4 V_t^3 e^{-\beta^2 V_t^2} dV_t$ with probability $P_2 = 1 - P_1$ [14]. Finally the pair (μ, V_t) is accepted with the probability given by (C) where $v_r = \sqrt{v_n^2 + V_t^2} - 2v_n V_t \mu$.

The SVT method in Geant4 has been recently revised and successfully benchmarked against Tripoli-4[®] [7]. In this work it has been again benchmarked with an emphasis on resonant heavy nuclei, here on ^{238}U , to validate the SVT algorithm which is the building block of the DBRC method. The default value of SVT.E.max has been increased from $400k_B T$ (~ 10.5 eV at 300 K) to 50 eV to use the SVT algorithm for the first three ^{238}U resonances. The Figures - left column - 2, 3 and 4 show that the energy of secondary neutrons

calculated with Geant4 agree well with Tripoli-4[®] within the statistical uncertainties. There is also an overall good agreement with MCNP6 for the energy-temperature combination for which the SVT algorithm is used in MCNP6. In fact the default energy threshold `SVT_E_max=400kBT` in MCNP6 could not have been changed in this work. These comparisons ensure that the SVT method is well implemented in Geant4 and allows to validate once again the building block of the DBRC algorithm for resonant heavy nuclei that is now studied.

3.2. DBRC method for resonant heavy nuclei

The assumption of the constant cross section leading to the SVT method is valid for light and medium nuclei since often their cross sections are constant at low energies. In the past it was assumed to be valid because it was thought that heavy nuclei do not significantly take part in the neutron slowing-down process. However it was shown [15, 16, 17] that the effect of low energy resonances should not be overlooked in resonant heavy nuclei especially for shielding and nuclear reactor applications. In fact, for example, Becker et al. [15] have demonstrated that treating exactly the elastic scattering kernel for the ²³⁸U resonances with DBRC instead of using the SVT assumption leads to a change of the k_{eff} value by as much as 350 pcm and Doppler coefficients by 16 % for an infinite array of identical fuel pin cells based on a PWR subassembly. It can also impact the extraction of resonance parameters from experimental data such as in [18].

To overcome the SVT approximation shortcoming, in the mid-1990s, Rothenstein and Dagan [19, 20] successfully developed scattering kernels for resonant nuclei in the epithermal region through the extension of $S(\alpha, \beta)$ tables to higher energy. The DBRC algorithm that is now considered has been firstly proposed by Rothenstein [21] and put again into light recently by Becker et al. [15]. To exactly sample the (μ, V_t) pair from Equation 2 on top of the SVT algorithm (Equation 3) another rejection loop/criterion (D) is added to get the exact Doppler Broadened elastic scattering kernel [22]:

$$p_{\text{DBRC}}(V_t, \mu) = C' p_{\text{SVT}}(V_t, \mu) \underbrace{\left(\frac{\sigma_0(v_r)}{\sigma_0^{\text{max}}(v_\xi)} \right)}_{(D)} \quad (4)$$

with C' a normalisation constant and $\sigma_0^{\text{max}}(v_\xi)$ the maximum 0 K cross section in the range $v_n \pm 4\sqrt{\frac{2k_B T}{M}}$. This range is chosen to be in accordance with the integral limits of the SIGMA-1 algorithm used for an exact Doppler broadening process [10]. From the rejection term (D), it can be seen, that the acceptance probability can be small near a resonance. Therefore this additional term increases the probability of selecting a velocity V_t that makes the neutron scattered at the resonance energy. This leads to a computation time increase because of the low acceptance probability.

The DBRC method has been implemented in `G4ParticleHPElasticFS::GetBiasedThermalNucleus` on top of the existing SVT algorithm as in previous works [15, 23, 24, 25]. To use and modify the behaviour of the DBRC algorithm in Geant4, the users have access to five new commands allowing to modify its behaviour as sketched in Figure 1:

- `/process/had/particle_hp/use_DBRC`
to enable (true) / disable (false) the DBRC algorithm. By default it is disabled.
- `/process/had/particle_hp/DBRC_A_min`
to set the minimum atomic mass in neutron masses for which the DBRC algorithm is applied. The default value is set to 200 amu.
- `/process/had/particle_hp/SVT_E_max`
to set the maximum energy up to which the SVT algorithm is used. The default value is set to $400k_B T$. The 0 K scattering kernel is used above the user defined value.
- `/process/had/particle_hp/DBRC_E_min(max)`
to set the minimum (maximum) energy between which the DBRC algorithm is applied. The default

value of `DBRC_min` is set to 0.1 eV, below the SVT algorithm is used. This value should corresponds to an energy below which there is no nuclear resonance for the considered isotopes. The default value of `DBRC_max` is set to 210 eV. These values are set in accordance with [23, 24].

The DBRC method being not implemented in the current MCNP6 release, the Geant4 DBRC results are only compared to Tripoli-4[®]. This latter has been validated by Zoia et al. [24] who have performed an exhaustive validation of its implementation against other ways to compute the Doppler broadening elastic scattering kernel such as the use of $S(\alpha, \beta)$ tables extended to higher energies [26], the Weight Correction Method (WCM) [27], or direct computation of the integral given by [28] in [29].

The thin-cylinder benchmark has been performed in the same conditions as for the SVT benchmark. The DBRC results presented in the right columns of Figures 2, 3 and 4 show a very good agreement between Geant4 and Tripoli-4[®] inside the statistical uncertainties. As can be seen, the secondary neutron energy distributions changes significantly compared to those obtained with the SVT method. Table 1, presenting the average scattered neutron energy, shows that the average energy with the SVT method remains the same for the different temperatures while with the DBRC method it increases with the temperature. Geant4 and Tripoli-4[®] agree well with each other since the relative errors are around 10^{-3} % for both SVT and DBRC methods. The average neutron energy increase agrees with the increase of the up-scattering probability (*i.e.* ratio of neutrons undergoing scattering with a higher energy than the initial neutron) as shown in Table 2. Again, here, the results between Geant4 and Tripoli-4[®] are in good agreement since the relative differences are less than 1%. All these results validate the DBRC algorithm implementation in Geant4.

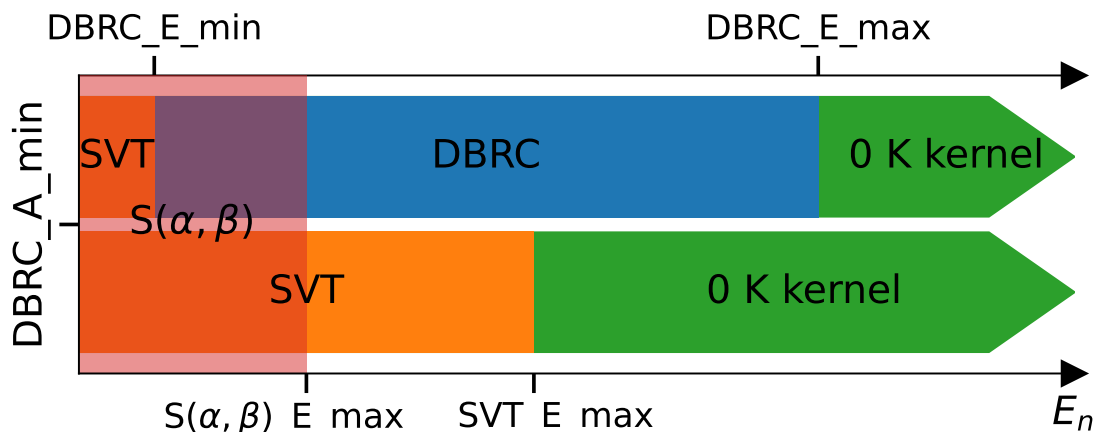


Figure 1: Doppler broadened elastic scattering final state models as a function of the neutron energy E_n . Bottom arrow : DBRC option switched off. Top arrow: DBRW option switched on.

SVT stands for Sampling of the Velocity of the Target nucleus, **DBRC** for Doppler Broadening Rejection Correction, $S(\alpha, \beta)$ for tables grasping the complex underlying physics of neutron-molecule or neutron-atom interactions and **0 K kernel** for elastic scattering with the assumption of zero velocity of the target nucleus. The default threshold values in Geant4 are: $S(\alpha, \beta)_E_{max}=4$ eV, $SVT_E_{max}=400k_B T$, $DBRC_E_{min}=0.1$ eV and $DBRC_E_{max}=210$ eV and $DBRC_A_{min}=200$ amu.

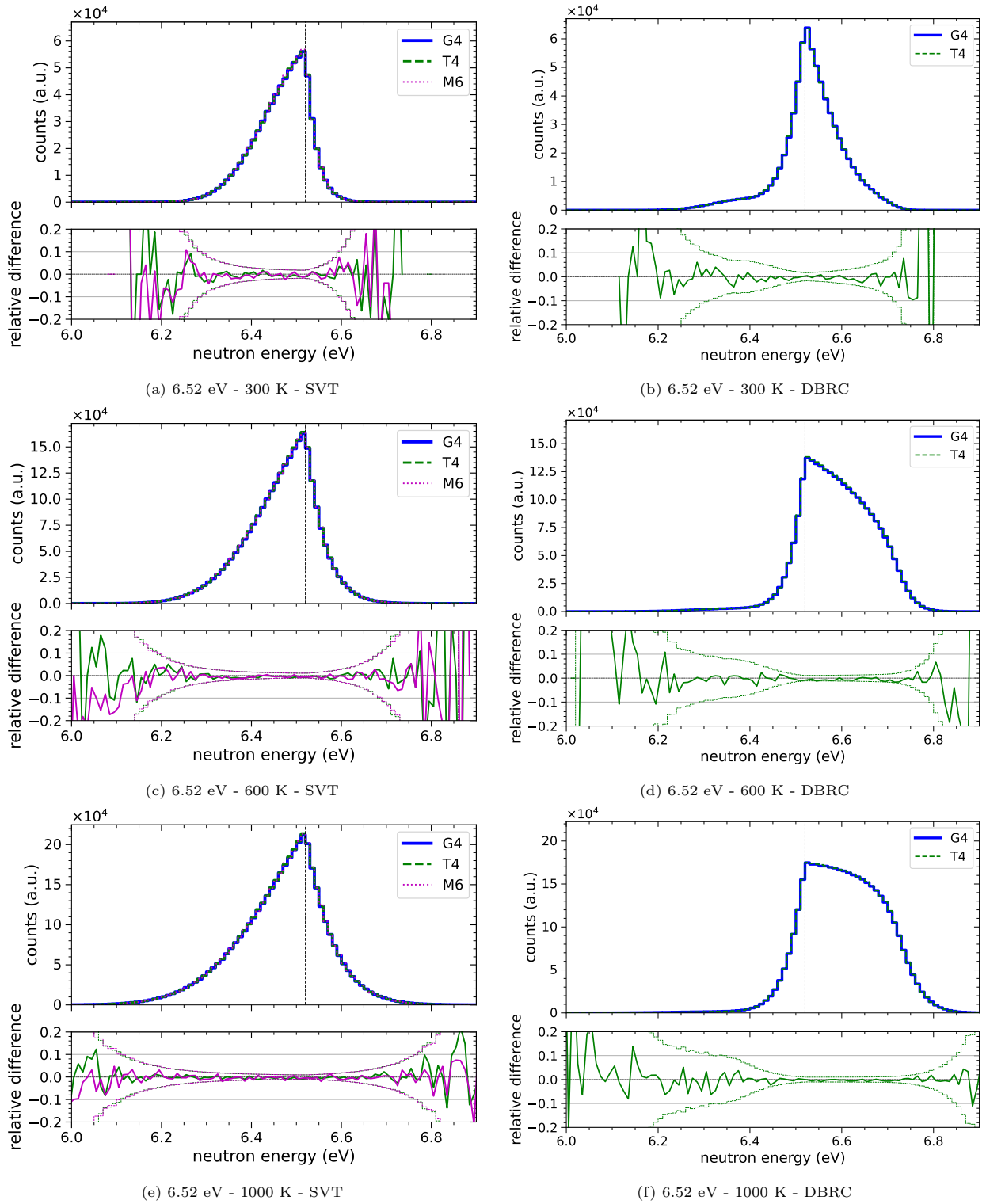


Figure 2: Outgoing neutron energy distributions of scattered neutrons for 6.52 eV neutrons on ^{238}U at different temperatures computed with SVT (left column) and DBRC (right column) computed with Geant4 and Tripoli-4[®]. The bottom part presents the relative difference G4/T4-1 (green solid line) and G4/M6-1 (magenta solid line) with three times the standard statistical error of this difference (dashed lines). MCNP6 results at 300 K and 1000 K have been normalised to Tripoli-4[®] ones, because the Doppler broadened cross sections at 300 K and 1000 K are effectively taken at 293.6 K and 900 K (pre-processed cross sections).

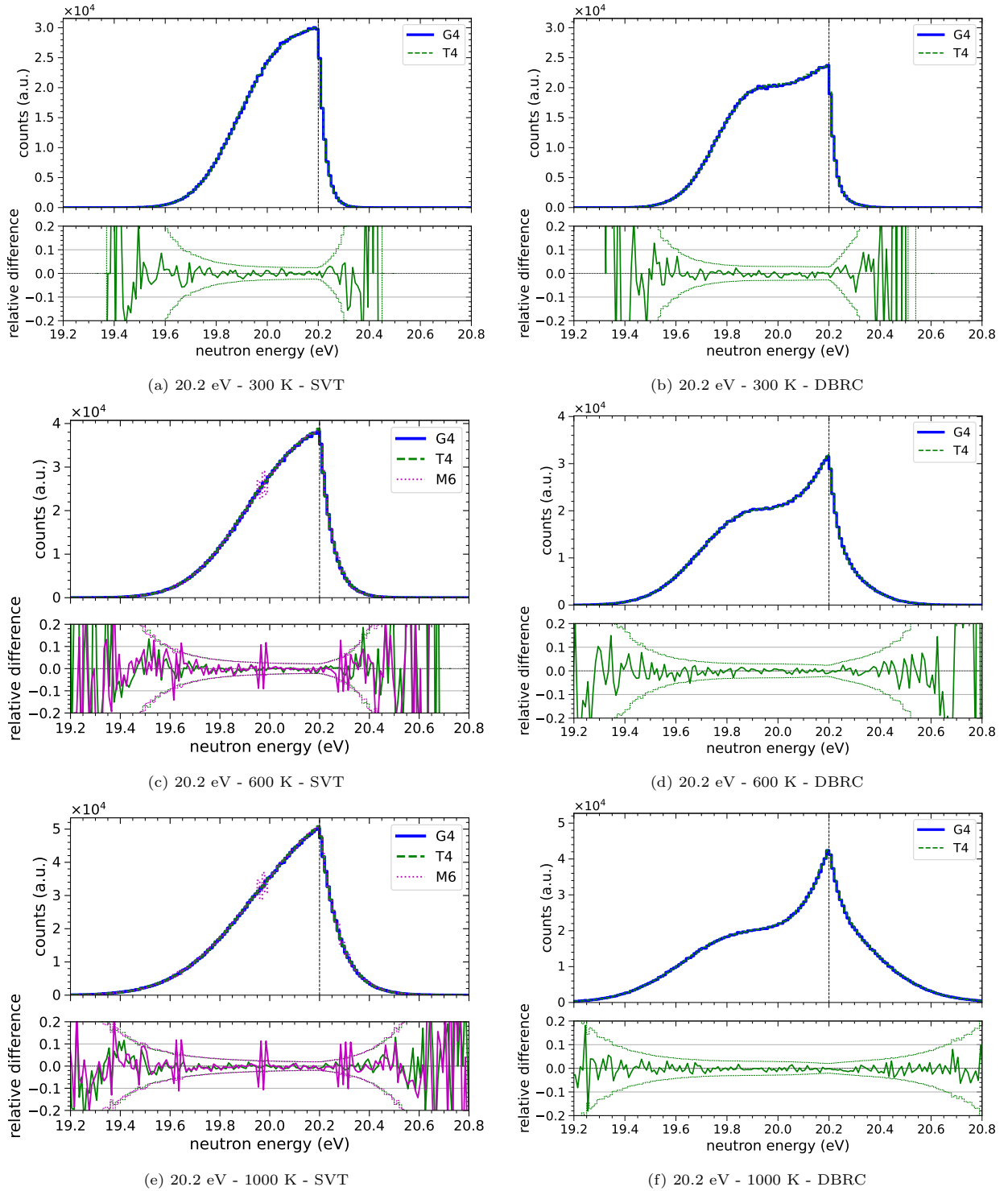
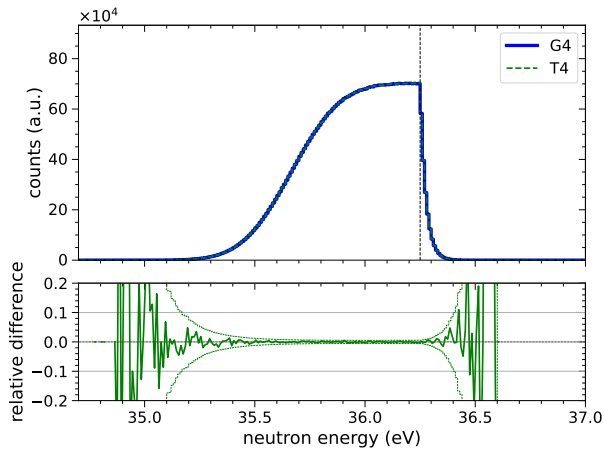
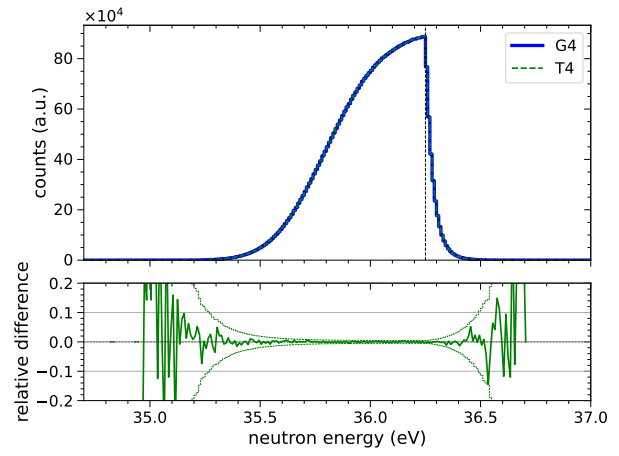


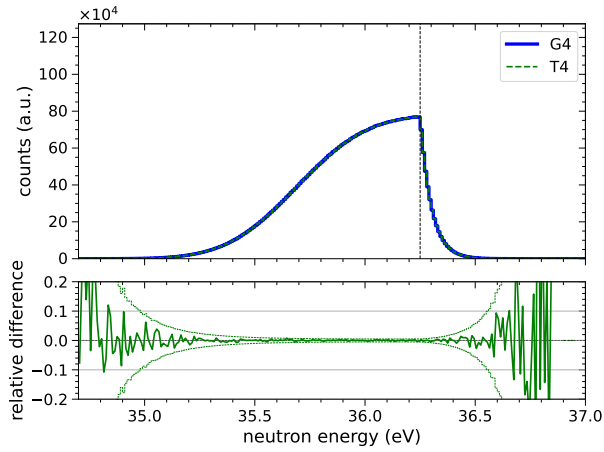
Figure 3: Outgoing neutron energy distributions of scattered neutrons for 20.2 eV neutrons on ^{238}U at different temperatures computed with SVT (left column) and DBRC (right column) computed with Geant4 and Tripoli-4[®]. The bottom part presents the relative difference G4/T4-1 (green solid line) and G4/M6-1 (magenta solid line) with three times the standard statistical error of this difference (dashed lines). MCNP6 results at 300 K and 1000 K have been normalised to Tripoli-4[®] ones, because the Doppler broadened cross sections at 300 K and 1000 K are effectively taken at 293.6 K and 900 K (pre-processed cross sections).



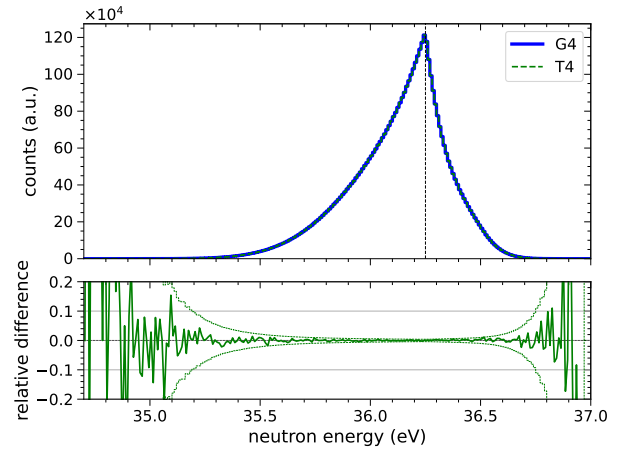
(a) 36.25 eV - 300 K - SVT



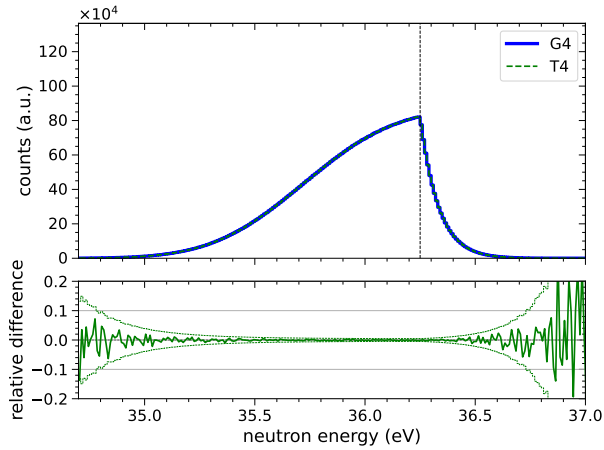
(b) 36.25 eV - 300 K - DBRC



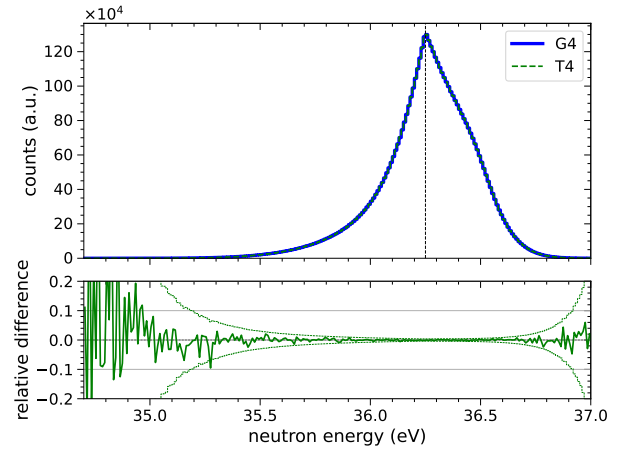
(c) 36.25 eV - 600 K - SVT



(d) 36.25 eV - 600 K - DBRC



(e) 36.25 eV - 1000 K - SVT



(f) 36.25 eV - 1000 K - DBRC

Figure 4: Outgoing neutron energy distributions of scattered neutrons for 36.25 eV neutrons on ^{238}U at different temperatures computed with SVT (left column) and DBRC (right column) computed with Geant4 and Tripoli-4[®]. The bottom part presents the relative difference $G4/T4-1$ (green solid line) with three times the standard statistical error of this difference (dashed line).

Table 1: Average energy of the scattered neutrons in eV for different primary energies and temperatures on ^{238}U with SVT and DBRC methods computed with Geant4 and Tripoli-4[®]. The relative difference (rel. diff.) between the two codes are in 10^{-3} %.

E (eV)	T (K)	Geant4		Tripoli-4 [®]		rel. diff.	
		SVT	DBRC	SVT	DBRC	SVT	DBRC
6.52	300	6.466	6.534	6.466	6.534	-0.85	-1.21
	600	6.466	6.589	6.466	6.589	-0.47	-0.62
	1000	6.467	6.605	6.467	6.605	-0.20	0.08
20.2	300	20.031	19.979	20.031	19.979	0.57	-0.69
	600	20.031	19.987	20.031	19.987	-0.22	1.40
	1000	20.032	20.043	20.032	20.044	0.75	-1.96
36.25	300	35.946	36.008	35.946	36.008	-0.02	-0.17
	600	35.946	36.128	35.946	36.128	-0.07	0.28
	1000	35.947	36.256	35.947	36.256	-0.08	0.02

Table 2: Up-scattering probability in % for different primary energies and temperatures on ^{238}U computed with SVT and DBRC methods with Geant4 and Tripoli-4[®]. The relative difference (rel. diff.) between the two codes are in %.

E (eV)	T (K)	Geant4		Tripoli-4 [®]		rel. diff.	
		SVT	DBRC	SVT	DBRC	SVT	DBRC
6.52	300	18.124	62.294	18.073	62.250	0.28	0.07
	600	25.452	82.798	25.437	82.832	0.06	-0.04
	1000	30.407	84.325	30.365	84.354	0.14	-0.03
20.2	300	7.499	5.692	7.470	5.681	0.38	0.20
	600	13.502	15.456	13.413	15.434	0.67	0.14
	1000	18.848	30.725	18.789	30.791	0.31	-0.21
36.25	300	4.242	7.135	4.236	7.143	0.15	-0.10
	600	8.264	30.658	8.265	30.629	-0.01	0.10
	1000	12.712	55.275	12.713	55.264	-0.01	0.02

4. On-the-fly cross section Doppler broadening in Geant4

In Monte Carlo neutron transport codes, cross sections can be Doppler broadened mainly with two methods. The first method consists in performing exactly the Doppler broadening (given by Equation 1) before the simulation for example with the SIGMA-1 algorithm implemented in a pre-processing tool such as NJOY [30]. Therefore no additional computation time is spent during the simulation for this. The drawbacks of this approach lies in the limited number of available temperatures for the simulation and the need to have a large computer memory size to store these data. It is mainly used in reference neutron transport codes such as Tripoli-4[®] and MCNP6. The second method is more demanding in terms of computational time since the Doppler broadening is done during the simulation, *i.e.* on-the-fly (OTF), but can be made at any temperature required by the user. This latter has been chosen in Geant4 for its versatility allowing to suit any needs from users coming from very different physics communities.

In comparing the thin-cylinder benchmark results from Geant4 and Tripoli-4[®], it was found that the total reaction rate from Geant4 was different from Tripoli-4[®], while relative values (such as the up-scattering probability) agree well between the two codes. This discrepancy arises because of the stochastic OTF Doppler broadening method implemented in Geant4. Its implementation can be seen, for example, in the G4ParticleHPElasticData::GetCrossSection method for elastic scattering and can be summarised as followed:

Listing 1: Pseudo-code of the implemented on-the-fly stochastic integral of the Doppler broadened cross section in Geant4.

```

///Initialization
size = max(10, T/60)

///On-the-fly stochastic integral computation
while ( $|\overline{\sigma_T^{\text{old}}(v_n)} - \overline{\sigma_T^{\text{new}}(v_n)}| > \epsilon_{\text{xs}} \cdot \overline{\sigma_T^{\text{old}}(v_n)}$ ) {
     $\overline{\sigma_T^{\text{old}}(v_n)} = \overline{\sigma_T^{\text{new}}(v_n)}$ 
    while (counter < size) {
        sample  $\mathbf{V}_t$  from Maxwell-Boltzmann distribution
        get  $\sigma(v_r)$ 
         $\overline{\sigma_T^{\text{new}}(v_n)} += \sigma(v_r) \cdot \frac{|\mathbf{V}_t - \mathbf{v}_n|}{v_n}$ 
        counter ++
    }
     $\overline{\sigma_T^{\text{new}}(v_n)} = \frac{\overline{\sigma_T^{\text{new}}(v_n)}}{\text{counter}}$ 
    size += size
}
return  $\overline{\sigma_T^{\text{new}}(v_n)}$ 

```

with *counter* the total number of loops performed by the algorithm and *size* the number of loops for each batch. At each step, the Doppler broadened cross section is computed and compared with its previous value. The algorithm stops when a convergence criterion ϵ_{xs} is met.

By default ϵ_{xs} are set to 0.03 and 0.01 respectively for capture and elastic reactions and for fission and inelastic reactions. However, these criteria do not guarantee sufficient cross section convergence as already pointed out in [31] and as can be seen in Figures 5a and 5b. Therefore the impact of ϵ_{xs} on the capture and elastic scattering has been studied with the thin-cylinder benchmark at 300 K and with 6.52 eV neutrons. The quantities of interest are the mean cross section, its standard deviation and its most probable value (MPV) since the distributions are not symmetric as can be seen in Figures 6a and 6b. The Geant4 OTF algorithm has been performed 8000 times to get statistical significant results for each convergence criterion. The results are compared to Tripoli-4[®] cross sections which have been computed exactly in using the SIGMA-1 algorithm with NJOY.

The Figures 5a and 5b, presenting the mean and MPV cross sections, show that the mean cross section converges when ϵ_{xs} decreases and that the MPV is always approximately the same for all convergence criterion values and is equal to the converged mean cross section value. With the default value $\epsilon_{\text{xs}}=0.03$, the mean capture and elastic cross sections are respectively around 2% and 10% lower than Tripoli-4[®] ones. For

$\epsilon_{\text{xs}} < 0.001$, the elastic and capture mean cross sections are converged to a value 1% higher than Tripoli-4[®] ones as shown in Figures 5a and 5b. This 1% discrepancy could be caused by interpolation errors since Geant4 results are compatible with Tripoli-4[®] cross sections taken at $6.520\text{eV} \pm 1\text{ meV}$. This discrepancy is therefore not investigated further.

The evolution of the cross section standard deviation is also quantified in Figure 7 as a function of ϵ_{xs} and shows a decrease from 23 % for elastic cross section (9% for capture) at $\epsilon_{\text{xs}} = 0.03$ to less than 1% for both cross sections for convergence criterion at $\epsilon_{\text{xs}} = 10^{-4}$. With these results, one can be tempted to change the default ϵ_{xs} value to a lower one, however a lower convergence criterion leads to a higher number of loops and therefore a higher computation time. In fact the computation time rises drastically as a function of ϵ_{xs} and then its increase starts to slow down from $\epsilon_{\text{xs}} = 10^{-4}$. In the future it could be worth to evaluate how this OTF algorithm performs compared to other algorithms such as the regression method [32, 33], the multipole representation of the cross section [34] or methods based on explicit treatment of target motion at collision sites [35].

It has to be pointed out that all the results presented in Section 3 have been computed with a convergence criterion set to $\epsilon_{\text{xs}} = 10^{-4}$ which is a trade-off between the cross section precision and computation time. Unfortunately this only can be done for benchmarking purposes, because of the prohibitive computation time for one OTF Doppler broadening algorithm call. However this problem would not be so important for integral studies since the Doppler broadening will be performed many times (at different energies) and so in average will give the right result.

It finally has to be recalled that this behaviour arises because the resonant part of the cross section is investigated. In fact for non-resonant cross sections, such as for ^1H , Figure 8 shows that the cross section mean and MPV are approximately the same for all convergence criteria and agree with Tripoli-4[®] cross sections. The capture cross section is again around 1 % higher, which could be caused by interpolation errors because the 0 K cross section for elastic scattering is almost constant at 6.52 eV, whereas the capture cross section significantly decreases. The standard deviation is under 1 % for elastic and 0.2 % for capture for the default convergence criteria as can be seen in Figures 9 and 10.

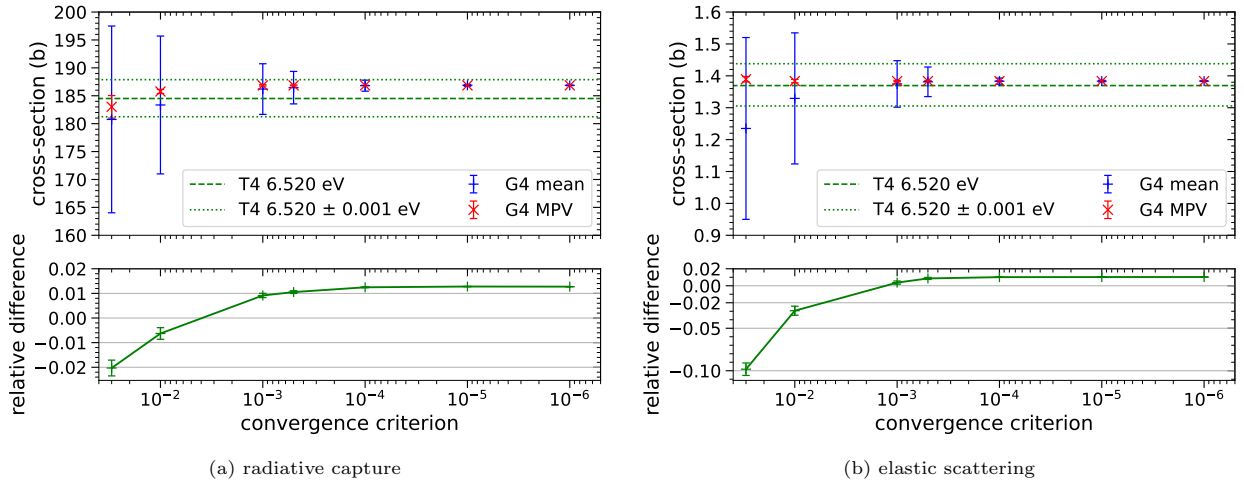


Figure 5: Mean and most probable value (MPV), along with their standard deviations, of the ^{238}U cross sections at 6.52 eV and 300 K as a function of the convergence criterion ϵ_{XS} calculated in Geant4 (G4). The cross section used in Tripoli-4[®] (T4) is shown as green dashed line. The cross section relative difference G4/T4-1 with its statistical error of the mean is shown at the bottom.

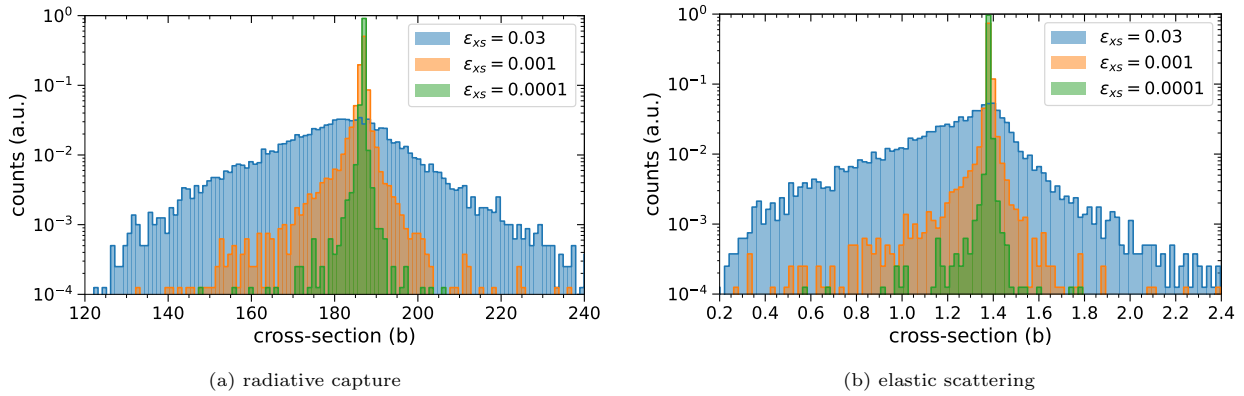


Figure 6: Normalised Doppler broadened cross section distributions for ^{238}U for different convergence criteria ϵ_{XS} .

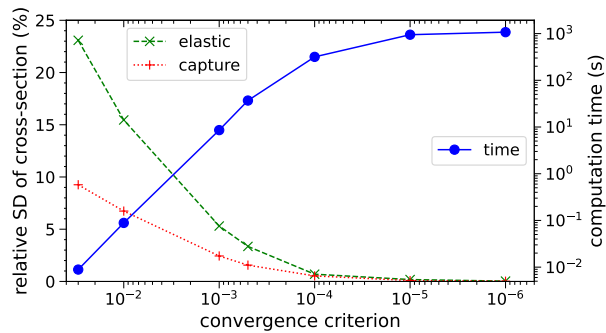


Figure 7: Relative standard deviation (SD) in % for elastic and capture ^{238}U cross sections and computation time for different convergence criteria ϵ_{XS} .

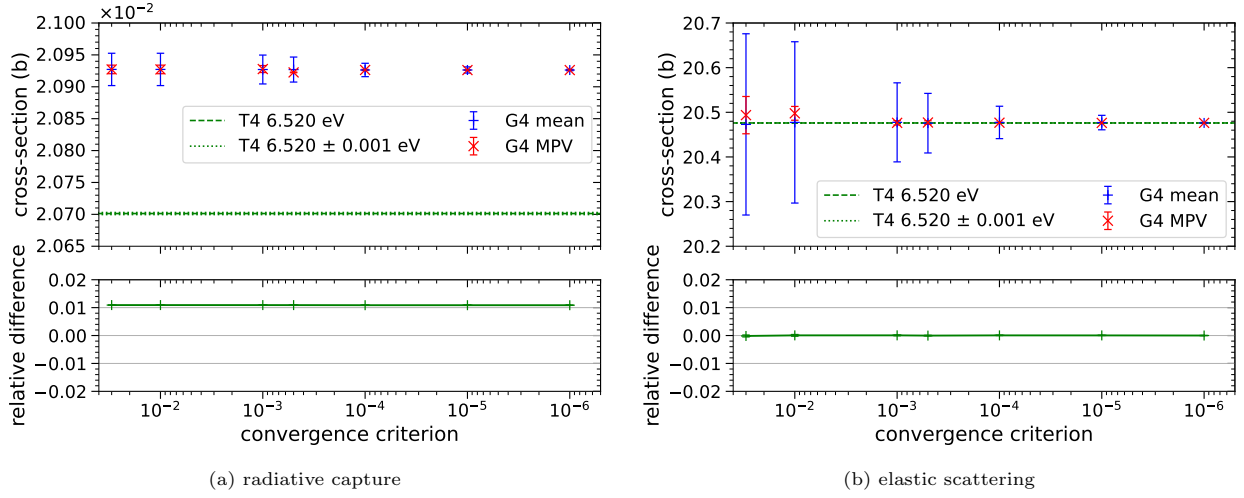


Figure 8: Mean and most probable value (MPV), along with their standard deviations, of the ^1H cross sections at 6.52 eV and 300 K as a function of the convergence criterion ϵ_{xs} calculated in Geant4 (G4). The cross section used in Tripoli-4[®] (T4) is shown as green dashed line. The cross section relative difference $G4/T4-1$ with its statistical error of the mean is shown at the bottom.

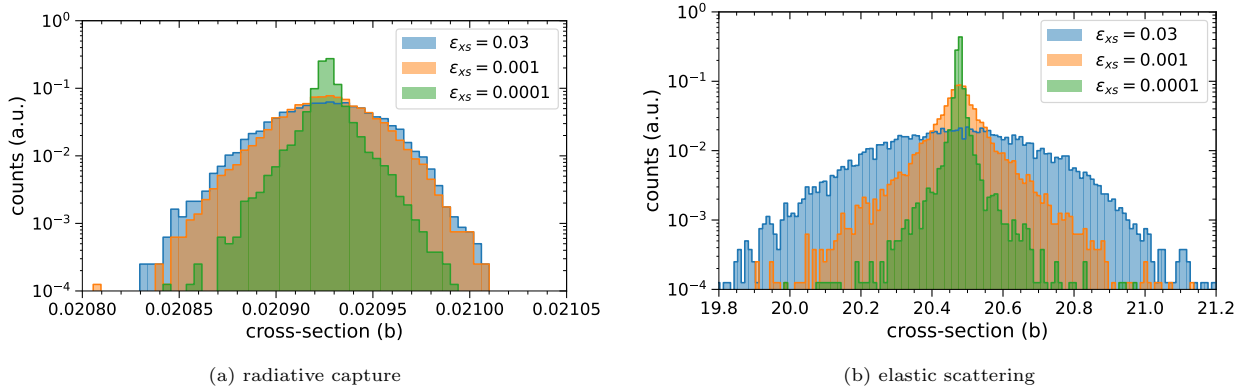


Figure 9: Normalised Doppler broadened cross section distributions for ^1H for different convergence criteria ϵ_{xs} .

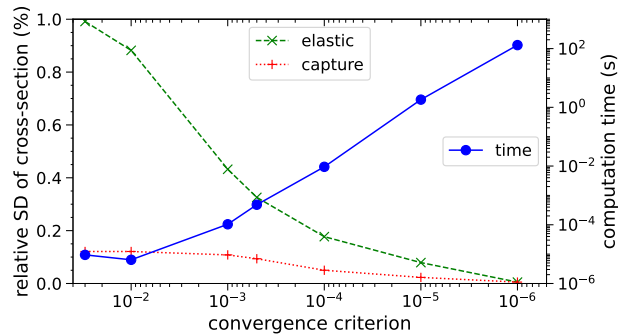


Figure 10: Relative standard deviation (SD) in % for elastic and capture ^1H cross sections and computation time for different convergence criteria ϵ_{xs} .

5. Conclusion

The Doppler Broadening Rejection Correction algorithm used to describe accurately the elastic scattering kernel of resonant heavy nuclei has been successfully implemented into Geant4. The validation performed with the reference Monte Carlo neutron transport code Tripoli-4[®] showed a very good agreement between the two codes within the statistical uncertainties. The DBRC algorithm will be implemented in the next Geant4 release. This work makes the Neutron-HP package at the state-of-the-art regarding the description of Doppler broadened elastic scattering kernels. The importance of the convergence criterion for the on-the-fly Doppler broadening routine has also been investigated and showed that the default convergence criterion values should be adapted on a simulation-by-simulation basis depending on the observable under study. With the developments performed in this work, the last missing feature in Geant4 compared to reference neutron transport codes is the description of the unresolved resonance region with probability tables. This last point will be addressed soon in a dedicated paper.

Acknowledgement

This work could be done thanks to the IAEA's technical cooperation programme, which supported a fellowship of Marek Zmeskal at IRFU, CEA in the framework of national project CZR0011 - Strengthening Human Resources Capacity in Nuclear Science and Technology. The authors wish to sincerely thank Cédric Jouanne and Alberto Ribon head of the Geant4 Hadronic Working Group for fruitful discussions respectively regarding Tripoli-4[®] and Geant4. Tripoli-4[®] is a registered trademark of CEA.

References

- [1] S. Agostinelli et al. Geant4—a simulation toolkit. *Nuclear Instruments and Methods in Physics Research Section A: Accelerators, Spectrometers, Detectors and Associated Equipment*, 506:250–303, 7 2003. ISSN 01689002. doi: 10.1016/S0168-9002(03)01368-8.
- [2] J. Allison et al. Geant4 developments and applications. *IEEE Transactions on Nuclear Science*, 53:270–278, 2 2006. ISSN 0018-9499. doi: 10.1109/TNS.2006.869826.
- [3] J. Allison et al. Recent developments in Geant4. *Nuclear Instruments and Methods in Physics Research Section A: Accelerators, Spectrometers, Detectors and Associated Equipment*, 835:186–225, nov 2016. ISSN 0168-9002. doi: 10.1016/J.NIMA.2016.06.125. URL <https://www.sciencedirect.com/science/article/pii/S0168900216306957>.
- [4] E. Mendoza et al. New standard evaluated neutron cross section libraries for the GEANT4 code and first verification. *IEEE Transactions on Nuclear Science*, 61:2357–2364, 2014. ISSN 00189499. doi: 10.1109/TNS.2014.2335538.
- [5] E. Mendoza, D. Cano-Ott, and R. Capote. Update of the Evaluated Neutron Cross Section Libraries for the Geant4 Code, IAEA technical report INDC(NDS)-0758 (releases JEFF-3.3, JEFF-3.2, ENDF/B-VIII.0, ENDF/B-VII.1, BROND-3.1 and JENDL-4.0u). Technical report, CIEMAT, Vienna, 2018. URL https://www-nds.iaea.org/geant4/figures/G4_10.04.p01_VS_MCNP6_ENDF80.pdf.
- [6] H. N. Tran et al. Comparison of the thermal neutron scattering treatment in MCNP6 and GEANT4 codes. *Nuclear Instruments and Methods in Physics Research Section A: Accelerators, Spectrometers, Detectors and Associated Equipment*, 893:84–94, jun 2018. ISSN 01689002. doi: 10.1016/j.nima.2018.02.094. URL <https://linkinghub.elsevier.com/retrieve/pii/S0168900218302651>.
- [7] L. Thulliez, C. Jouanne, and E. Dumonteil. Improvement of Geant4 Neutron-HP package: From methodology to evaluated nuclear data library. *Nuclear Instruments and Methods in Physics Research Section A: Accelerators, Spectrometers, Detectors and Associated Equipment*, 1027:166187, 3 2022. ISSN 01689002. doi: 10.1016/j.nima.2021.166187.
- [8] E. Brun et al. TRIPOLI-4[®], CEA, EDF and AREVA reference Monte Carlo code. *Annals of Nuclear Energy*, 82:151–160, 8 2015. ISSN 03064549. doi: 10.1016/j.anucene.2014.07.053.
- [9] C. J. Werner et al. MCNP Version 6.2 Release Notes, 2 2018.
- [10] D. E. Cullen. Program SIGMA1 (version 79-1): Doppler broaden evaluated cross sections in the evaluated nuclear data file/version B (ENDF/B) format, 10 1979.
- [11] I. Duhamel et al. International Criticality Benchmark Comparison for Nuclear Data Validation. *Transactions of the American Nuclear Society*, 121, 2019.
- [12] M. B. Chadwick et al. ENDF/B-VII.1 Nuclear Data for Science and Technology: Cross Sections, Covariances, Fission Product Yields and Decay Data. *Nuclear Data Sheets*, 112:2887–2996, 12 2011. ISSN 00903752. doi: 10.1016/j.nds.2011.11.002.
- [13] M. Zmeskal and L. Thulliez. Geant4 Neutron-HP benchmarking application, 2023. URL https://gitlab.com/lthullie/geant4_neutronhp_benchmarkapp.
- [14] R. R. Coveyou, R. R. Bate, and R. K. Osborn. Effect of moderator temperature upon neutron flux in infinite, capturing medium. *Journal of Nuclear Energy (1954)*, 2:153–167, 1 1956. ISSN 08913919. doi: 10.1016/0891-3919(55)90030-9.

- [15] B. Becker, R. Dagan, and G. Lohnert. Proof and implementation of the stochastic formula for ideal gas, energy dependent scattering kernel. *Annals of Nuclear Energy*, 36:470–474, 5 2009. ISSN 03064549. doi: 10.1016/j.anucene.2008.12.001.
- [16] R. Dagan and C. H. M. Broeders. On the effect of Resonance dependent Scattering-kernel on Fuel cycle and inventory. 9 2006.
- [17] R. Dagan, B. Becker, Y. Danon, M. Rapp, D. Barry, and G. Lohnert. Modelling Resonance Dependent Angular Distribution via DBRC in Monte Carlo Codes. *Journal of the Korean Physical Society*, 59:983–986, 8 2011. ISSN 0374-4884. doi: 10.3938/jkps.59.983.
- [18] F. Gunsing and E. Berthoumieux et al. Measurement of resolved resonances of $^{232}\text{Th}(n,\gamma)$ at the n-TOF facility at CERN. *Physical Review C*, 85, 6 2012. ISSN 1089490X. doi: 10.1103/PHYSREVC.85.064601.
- [19] W. Rothenstein and R. Dagan. Ideal gas scattering kernel for energy dependent cross-sections. *Annals of Nuclear Energy*, 25:209–222, 3 1998. ISSN 03064549. doi: 10.1016/S0306-4549(97)00063-7. URL <https://linkinghub.elsevier.com/retrieve/pii/S0306454997000637>.
- [20] W. Rothenstein. Proof of the formula for the ideal gas scattering kernel for nuclides with strongly energy dependent scattering cross sections. *Annals of Nuclear Energy*, 31:9–23, 1 2004. ISSN 03064549. doi: 10.1016/S0306-4549(03)00216-0. URL <https://linkinghub.elsevier.com/retrieve/pii/S0306454903002160>.
- [21] W. Rothenstein. Proceedings of the ENS Conference Tel Aviv, 1994.
- [22] W. Rothenstein and R. Dagan. Two-body kinetics treatment for neutron scattering from a heavy Maxwellian gas. *Annals of Nuclear Energy*, 22:723–730, 11 1995. ISSN 03064549. doi: 10.1016/0306-4549(95)00002-A.
- [23] E. E. Sunny, F. B. Brown, B. C. Kiedrowski, and W. Martin. Temperature effects of resonance scattering for epithermal neutrons in MCNP. pages 803–811, 4 2012.
- [24] A. Zoia, E. Brun, C. Jouanne, and F. Malvagi. Doppler broadening of neutron elastic scattering kernel in Tripoli-4 $\text{\textcircled{R}}$. *Annals of Nuclear Energy*, 54:218–226, 4 2013. ISSN 03064549. doi: 10.1016/j.anucene.2012.11.023.
- [25] F. B. Brown. Doppler Broadening Resonance Correction for Free-gas Scattering in MCNP6.2, 5 2019.
- [26] R. Dagan. On the use of $S(\alpha, \beta)$ tables for nuclides with well pronounced resonances. *Annals of Nuclear Energy*, 32:367–377, 3 2005. ISSN 03064549. doi: 10.1016/j.anucene.2004.11.003.
- [27] D. Lee, K. Smith, and J. Rhodes. The impact of ^{238}U resonance elastic scattering approximations on thermal reactor Doppler reactivity. *Annals of Nuclear Energy*, 36:274–280, 4 2009. ISSN 03064549. doi: 10.1016/j.anucene.2008.11.026.
- [28] M. Ouisloumen and R. Sanchez. A Model for Neutron Scattering Off Heavy Isotopes That Accounts for Thermal Agitation Effects. *Nuclear Science and Engineering*, 107:189–200, 3 1991. ISSN 0029-5639. doi: 10.13182/NSE89-186.
- [29] S. Z. Ghayeb, M. Ouisloumen, A. M. Ougouag, and K. N. Ivanov. Deterministic modeling of higher angular moments of resonant neutron scattering. *Annals of Nuclear Energy*, 38:2291–2297, 10 2011. ISSN 03064549. doi: 10.1016/j.anucene.2011.04.025.
- [30] R. Macfarlane, D. W. Muir, R. M. Boicourt, A. C. Kahler, and J. L. Conlin. The NJOY Nuclear Data Processing System, Version 2016, 1 2017.
- [31] X. X. Cai, I. Llamas-Jansa, and B. C. Hauback. Accuracy and speed of the HP models. 7 2014. URL https://indico.cern.ch/event/319884/contributions/1698321/attachments/616390/848181/Geant4_neutron_workshop.pdf.
- [32] G. Yesilyurt, W. R. Martin, and F. B. Brown. On-the-Fly Doppler Broadening for Monte Carlo Codes. *Nuclear Science and Engineering*, 171:239–257, 7 2012. ISSN 0029-5639. doi: 10.13182/NSE11-67.
- [33] W. R. Martin, F. B. Brown, S. Wilderman, and G. Yesilyurt. On-The-Fly Neutron Doppler Broadening in MCNP. page 03102. EDP Sciences, 6 2014. ISBN 978-2-7598-1269-1. doi: 10.1051/snamc/201403102.
- [34] B. Forget, S. Xu, and K. Smith. Direct Doppler broadening in Monte Carlo simulations using the multipole representation. *Annals of Nuclear Energy*, 64:78–85, 2 2014. ISSN 03064549. doi: 10.1016/j.anucene.2013.09.043.
- [35] T. Viitanen and J. Leppänen. Explicit Treatment of Thermal Motion in Continuous-Energy Monte Carlo Tracking Routines. *Nuclear Science and Engineering*, 171:165–173, 6 2012. ISSN 0029-5639. doi: 10.13182/NSE11-36.